

## Structure and magnetism of V-doped SnO<sub>2</sub> thin films: effect of the substrate

This article has been downloaded from IOPscience. Please scroll down to see the full text article.

2007 J. Phys.: Condens. Matter 19 256204

(<http://iopscience.iop.org/0953-8984/19/25/256204>)

View [the table of contents for this issue](#), or go to the [journal homepage](#) for more

Download details:

IP Address: 129.252.86.83

The article was downloaded on 28/05/2010 at 19:22

Please note that [terms and conditions apply](#).

## Structure and magnetism of V-doped SnO<sub>2</sub> thin films: effect of the substrate

Jun Zhang<sup>1,2</sup>, R Skomski<sup>1,2</sup>, L P Yue<sup>1,2</sup>, Y F Lu<sup>2,3</sup> and D J Sellmyer<sup>1,2</sup>

<sup>1</sup> Department of Physics and Astronomy, University of Nebraska, Lincoln, NE 68588, USA

<sup>2</sup> Nebraska Center for Materials and Nanoscience, University of Nebraska, Lincoln, NE 68588, USA

<sup>3</sup> Department of Electrical Engineering, University of Nebraska, Lincoln, NE 68588, USA

Received 15 April 2007

Published 5 June 2007

Online at [stacks.iop.org/JPhysCM/19/256204](http://stacks.iop.org/JPhysCM/19/256204)

### Abstract

We report on the structure and magnetism of V-doped SnO<sub>2</sub> thin films grown by pulsed laser deposition. The structure and magnetic properties of the films strongly depend on the substrates on which the films are grown. Films grown on Al<sub>2</sub>O<sub>3</sub> substrates are single crystalline and show anisotropic in-plane magnetic moments, while films grown on Si substrates are nanocrystalline and show no anisotropy. Compared with that of single-crystalline films, the magnetic moment of nanocrystalline films is higher at low V concentration, decreases more quickly as the V concentration increases, and is more sensitive to vacuum annealing. Our results suggest important roles for spin-orbit coupling and defects in the magnetism of diluted magnetic oxides.

High-temperature magnetic oxide semiconductors have attracted much attention in spin electronics, because they combine optical transparency and semiconductivity with ferromagnetism above room temperature. Motivated by theoretical predictions [1, 2], much work has been done on the transition-metal doped oxides in which room-temperature ferromagnetism has been observed, including ZnO [3], TiO<sub>2</sub> [4, 5] and SnO<sub>2</sub> [6–8]. However, compared with the booming materials research on the magnetic oxide semiconductors, the understanding of their magnetism is still in its infancy, with an ongoing debate about intrinsic ferromagnetism and extrinsic magnetic properties. Although the F-centre model [7] has been proposed to explain the intrinsic ferromagnetism, recent experimental results suggest that the magnetism of magnetic oxide semiconductors is very complicated and may involve other effects. One example is giant magnetic moments, such as the room-temperature moment of 7.5  $\mu_B$ /Co found in Co-doped SnO<sub>2</sub> [6], and 4.23  $\mu_B$ /V in V-doped TiO<sub>2</sub> thin films [9]. Another interesting observation is the anisotropy of the magnetic moment observed in Co-doped ZnO [10]. Both phenomena suggest an important role of spin-orbit coupling in the ferromagnetism of the ferromagnetic oxide semiconductors. Moreover, the magnetism of the doped oxides strongly depends on crystalline defects. Recently, Kaspar *et al* [11] found that structurally defective Cr-doped TiO<sub>2</sub> thin films show high-temperature ferromagnetism, but

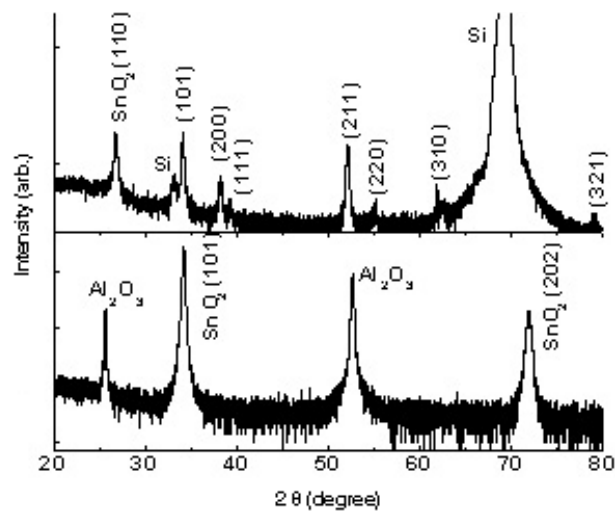


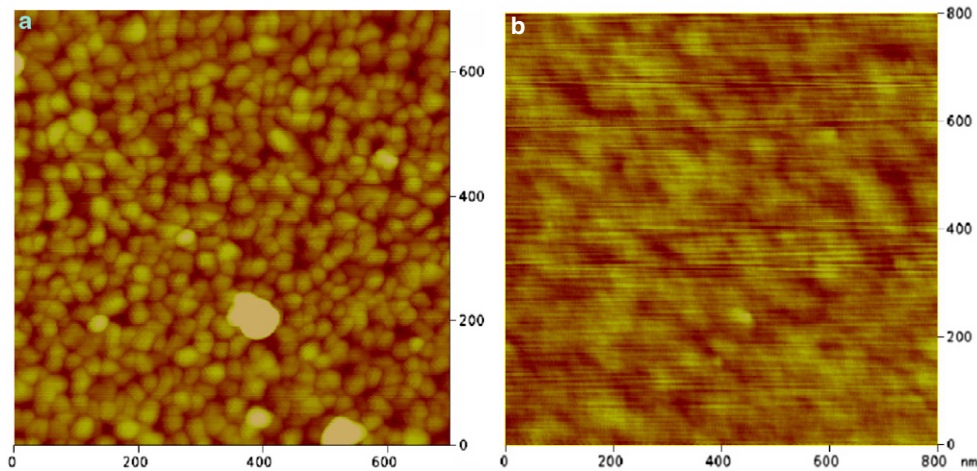
**Figure 1.** XRD patterns of the  $\text{Sn}_{1-x}\text{V}_x\text{O}_2$  ( $x = 0.10$ ) thin films grown on Si (top panel) and  $\text{Al}_2\text{O}_3$  (bottom panel) substrates.

those with excellent structural quality do not. The investigation of these phenomena will help to understand the intriguing ferromagnetism in doped oxides.

In this paper we investigate the structure and magnetic properties of V-doped  $\text{SnO}_2$  thin films. The films show not only room-temperature ferromagnetism but also a pronounced anisotropy of the magnetic moment, and the magnetic properties strongly depend on the substrates on which the films are grown. Strong in-plane anisotropic magnetic moments are observed in the single-crystalline films grown on sapphire substrates but not in the polycrystalline films grown on silicon substrates. The films grown on different substrates have different magnetic moments and their magnetic properties show different sensitivities to vacuum annealing.

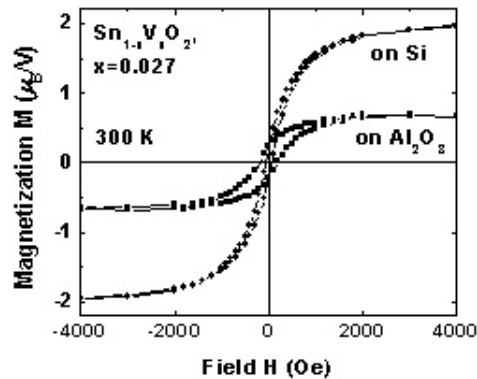
V-doped  $\text{SnO}_2$  ( $\text{Sn}_{1-x}\text{V}_x\text{O}_2$ ,  $x = 0-0.10$ ) thin films were grown on Si(001) and r-cut  $\text{Al}_2\text{O}_3(1\bar{1}02)$  substrates by a pulsed laser deposition (PLD) method.  $\text{Sn}_{1-x}\text{V}_x\text{O}_2$  ceramic targets were prepared by standard solid state reaction of  $\text{SnO}_2$  (99.9% purity) and  $\text{V}_2\text{O}_5$  (99.995% purity) powders. The base pressure of the PLD chamber was  $3 \times 10^{-7}$  Torr. The oxygen pressure during film growth was kept at  $5 \times 10^{-4}$  Torr and the substrate temperature was 600 °C. The film thickness was about 50 nm. The composition of the films was determined by energy dispersive x-ray spectroscopy, and the structures were characterized by x-ray diffraction (XRD) and atomic force microscopy (AFM). The magnetic measurements were made in a superconducting quantum interference device (SQUID) magnetometer (Quantum Design, MPMS-XL).

Figure 1 shows the XRD patterns of the  $\text{Sn}_{1-x}\text{V}_x\text{O}_2$  ( $x = 0.10$ ) thin films grown on Si (top panel) and  $\text{Al}_2\text{O}_3$  (bottom panel) substrates, respectively. The XRD patterns indicate that both of the films are of rutile structure; the film grown on the Si substrate is polycrystalline with random orientation, while the film grown on the  $\text{Al}_2\text{O}_3$  substrate has (101) orientation. Pole figure results (not shown) further revealed that the film grown on  $\text{Al}_2\text{O}_3$  is single crystal and is epitaxially grown with its [010] axis along the  $[\bar{1}2]10$  direction of the  $\text{Al}_2\text{O}_3$  substrate, consistent with the result in [12]. The (101) plane spacing of the films grown on  $\text{Al}_2\text{O}_3$  decreases almost linearly as the V concentration increases, suggesting that at least some V goes into the  $\text{SnO}_2$  lattice and substitutes for Sn.



**Figure 2.** AFM images of the  $\text{Sn}_{1-x}\text{V}_x\text{O}_2$  ( $x = 0.10$ ) thin films grown on Si (a) and  $\text{Al}_2\text{O}_3$  (b) substrates.

(This figure is in colour only in the electronic version)



**Figure 3.** Field-dependent magnetization curves at 300 K for the  $\text{Sn}_{1-x}\text{V}_x\text{O}_2$  ( $x = 0.027$ ) thin films grown on Si and  $\text{Al}_2\text{O}_3$  substrates.

The films were further characterized by AFM. AFM images of the  $\text{Sn}_{1-x}\text{V}_x\text{O}_2$  ( $x = 0.10$ ) thin films grown on Si and  $\text{Al}_2\text{O}_3$  substrates are shown in figure 2. The film grown on Si is nanocrystalline, with an average grain size of about 20–30 nm and a surface roughness of about 1.5 nm. The film grown on  $\text{Al}_2\text{O}_3$  does not show any granular features and is much flatter (roughness of 0.3 nm), consistent with the epitaxy and single-crystalline quality revealed by the XRD results.

Room-temperature ferromagnetism was observed in the  $\text{Sn}_{1-x}\text{V}_x\text{O}_2$  thin films grown on both Si and  $\text{Al}_2\text{O}_3$  substrates. Figure 3 shows typical field-dependent magnetization curves measured at 300 K in  $\text{Sn}_{1-x}\text{V}_x\text{O}_2$  ( $x = 0.027$ ) thin films grown on Si and  $\text{Al}_2\text{O}_3$  substrates, respectively, with the magnetic field applied in the plane of the film. The diamagnetic contributions from substrates were subtracted. The film grown on the  $\text{Al}_2\text{O}_3$  substrate shows an open hysteresis loop with a considerable remanent magnetization (about 30% of the saturation magnetization) and a coercive field of 200 Oe, indicating the presence of strong ferromagnetic

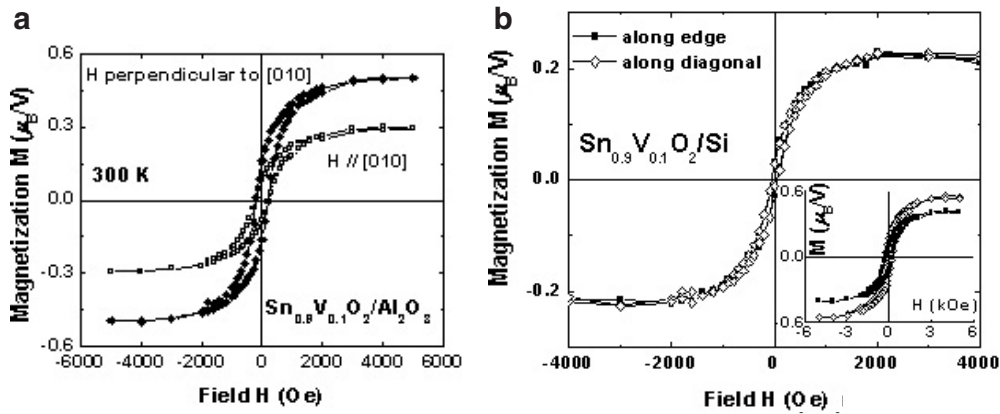


**Figure 4.** Hysteresis loops: (a) at 300 K for the  $\text{Sn}_{1-x}\text{V}_x\text{O}_2$  ( $x = 0.10$ ) thin film grown on an  $\text{Al}_2\text{O}_3$  substrate, with field parallel and perpendicular to the [010] direction, and (b) at 300 K for the  $\text{Sn}_{1-x}\text{V}_x\text{O}_2$  ( $x = 0.10$ ) thin films grown on Si and  $\text{Al}_2\text{O}_3$  (inset) substrates, with field along the edge (solid square) and diagonal (open diamond) of the square samples.

ordering. Although the film grown on the Si substrate has smaller remanent magnetization and coercive field than the film grown on the  $\text{Al}_2\text{O}_3$  substrate, it shows a higher magnetic moment.

The finding that the nanocrystalline film shows stronger ferromagnetism than the single-crystalline film suggests that the defect structure plays an important role in the ferromagnetism. Compared with the single-crystalline thin film grown on  $\text{Al}_2\text{O}_3$  substrate, the nanocrystalline  $\text{Sn}_{1-x}\text{V}_x\text{O}_2$  thin film must have significantly more structural defects, such as lattice defects at grain boundaries. Grain boundary defects have been implicated to play an important role in the ferromagnetism of doped magnetic oxide semiconductors. Originally paramagnetic Co-doped  $\text{TiO}_2$  nanocrystals became weakly ferromagnetic when aggregated and strongly ferromagnetic when spin-coated into nanocrystalline films [13]. Similar results were also reported in a Ni-doped ZnO nanocrystal system [14]. Recently, the Chambers group [11] reported that ferromagnetism is limited in fast-grown Cr-doped  $\text{TiO}_2$  thin films but does not occur in slowly grown thin films, and correlated the ferromagnetism to structural defects others than those introduced to maintain charge neutrality.

The most remarkable observation in the  $\text{Sn}_{1-x}\text{V}_x\text{O}_2$  thin films is that the *in-plane* magnetic moment of the film grown on  $\text{Al}_2\text{O}_3$  substrate is strongly anisotropic. Figure 4(a) shows the two hysteresis loops at 300 K of a  $\text{Sn}_{1-x}\text{V}_x\text{O}_2$  ( $x = 0.10$ ) thin film grown on  $\text{Al}_2\text{O}_3$  substrate with the applied magnetic field parallel and perpendicular to the [010] direction, respectively. The saturation moments of the two hysteresis loops are obviously different: that with the field perpendicular to the [010] direction is about 40% higher than that with the field parallel to the [010] direction.

The in-plane anisotropy was not observed in the films grown on the Si substrate, which consist of randomly oriented nanocrystalline grains. Figure 4(b) shows the hysteresis loops for the V-doped  $\text{SnO}_2$  thin films ( $x = 0.10$ ) grown on Si and  $\text{Al}_2\text{O}_3$  (inset) substrates. Since the film grown on the Si substrate is randomly oriented, we compare the loops measured with the applied magnetic field along an edge and along a diagonal of the square samples. One can clearly see that in the case of the film grown on  $\text{Al}_2\text{O}_3$  the saturation magnetic moments measured along different directions are obviously different; but such anisotropy is absent in the film grown on Si, in which the two loops are almost identical. The in-plane character of the measurement shows that the anisotropy of magnetic moments is an intrinsic property rather

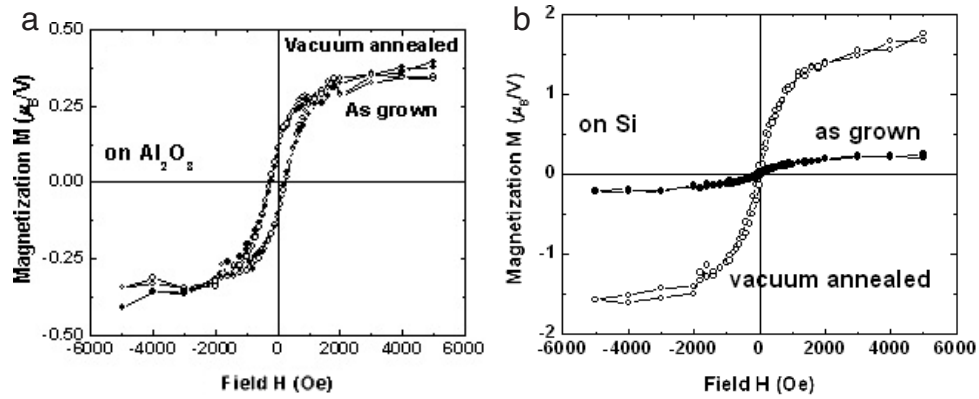


**Figure 5.** Hysteresis loops at 300 K for the  $\text{Sn}_{1-x}\text{V}_x\text{O}_2$  ( $x = 0.05$ ) thin films grown on (a)  $\text{Al}_2\text{O}_3$  and (b) Si substrates before (solid circles) and after (open circles) 3 h of vacuum annealing at  $500^\circ\text{C}$ .

than a sample-shape effect. The in-plane anisotropy is limited to single-crystalline films grown on  $\text{Al}_2\text{O}_3$ , as contrasted to polycrystalline films grown on Si, because the random orientation of the grains in nanocrystalline films averages the net anisotropy to zero.

The anisotropy of the magnetic moment may arise from spin-orbit coupling. It is known that the spin-orbit interaction creates an anisotropic orbital-moment contribution [15], and Zaránd *et al* [16] proposed that in  $\text{Ga}_{1-x}\text{Mn}_x\text{As}$ , because of spin-orbit coupling, the effective Mn-Mn ferromagnetic interaction is strongly anisotropic and the neighbouring Mn spins tend to be aligned along a certain direction. They argued that the results apply to other magnetic semiconductors with strong spin-orbit interaction. Heavy elements, like Sn in the  $\text{Sn}_{1-x}\text{V}_x\text{O}_2$  studied here, favour spin-orbit coupling, and one may therefore expect to see the anisotropic magnetic moments in the present  $\text{Sn}_{1-x}\text{V}_x\text{O}_2$  thin films. The anisotropic moment observed in Co-doped ZnO has also been related to orbital moment [10].

By comparing figures 3 and 4(b), we find that the magnetic moment decreases with increasing V doping level, but the drop in the case of the nanocrystalline films is much more significant than that of the single-crystalline films. As shown in figure 4(b) and its inset, for the films doped with 10% V, the nanocrystalline film shows a lower magnetic moment than the single-crystalline film, which is different from the results for films with lower V concentration indicated by figure 3. The trend towards lower moments at higher doping levels is commonly observed in dilute magnetic oxides. It may be attributed to the formation of dopant pairs or clusters that are antiferromagnetically coupled and yield little or no contribution to the total moment [10]. Moreover, in the nanocrystalline films, as the V content increases, V may aggregate at grain boundaries, which further reduces the magnetic moment of the nanocrystalline films compared with the single-crystalline films.

Finally, we compare the vacuum annealing effect on the ferromagnetism of the  $\text{Sn}_{1-x}\text{V}_x\text{O}_2$  thin films grown on different substrates. The  $\text{Sn}_{1-x}\text{V}_x\text{O}_2$  ( $x = 0.05$ ) thin films grown on  $\text{Al}_2\text{O}_3$  and Si substrates were annealed in a vacuum (better than  $1 \times 10^{-7}$  Torr) at  $500^\circ\text{C}$  for 3 h. Figure 5 shows the field-dependent magnetization curves measured before and after annealing. Vacuum annealing had a very weak effect on the magnetization of the film grown on the  $\text{Al}_2\text{O}_3$  substrate, but dramatically enhanced the ferromagnetism of the film grown on the Si substrate. Although the mechanism for the ferromagnetic ordering in the ferromagnetic oxide semiconductors is still not well understood, it is believed that carriers (in the cases of

most oxides, electrons) [17] and/or oxygen vacancies [7] play important roles in producing ferromagnetism. Vacuum annealing may remove oxygen atoms, creating oxygen vacancies and extra electrons, and, therefore, favour ferromagnetism. In the nanocrystalline  $\text{Sn}_{1-x}\text{V}_x\text{O}_2$  thin films with loosely connected grains and large surface areas (see figure 2), oxygen atoms may diffuse out more efficiently during vacuum annealing than in the single-crystalline thin films. So vacuum annealing has a stronger effect on the nanocrystalline  $\text{Sn}_{1-x}\text{V}_x\text{O}_2$  thin films grown on Si than the single crystalline ones grown on  $\text{Al}_2\text{O}_3$ .

In summary, we have observed room-temperature ferromagnetism in V-doped  $\text{SnO}_2$  thin films. The ferromagnetic properties strongly depend on the substrates on which the films are grown, and therefore, on the structure of the films. Anisotropic magnetic moments were observed in the plane of the film in the single-crystalline thin films grown on the  $\text{Al}_2\text{O}_3$  substrate but not in the nanocrystalline films grown on the Si substrate. Vacuum annealing has a stronger effect on the ferromagnetism of the nanocrystalline films than that of the single-crystalline films. The results suggest that spin-orbit coupling and defects play important roles in the magnetism of dilute magnetic oxides.

### Acknowledgments

This research is supported by the US National Science Foundation Materials Research Science and Engineering Center (NSF-MRSEC), the W M Keck foundation and the Nebraska Center of Materials and Nanoscience (NCMN).

### References

- [1] Dietl T, Ohno H, Matsukura F, Cibert J and Ferrand D 2000 *Science* **287** 1019
- [2] Sato K and Katayama-Yoshida H 2000 *Japan. J. Appl. Phys.* **2** **39** L555
- [3] Ueda K, Tabata H and Kawai T 2001 *Appl. Phys. Lett.* **79** 988
- [4] Matsumoto Y, Murakami M, Shono T, Hasegawa T, Furumura T, Kawasaki M, Ahmet P, Chikyow T, Koshihara S and Koinuma H 2001 *Science* **291** 854
- [5] Chambers S A, Thevuthasan S, Farrow R F, Marks R F, Thiele J U, Folks L, Samant M G, Kellock A J, Ruzycski N, Ederer D L and Diebond U 2001 *Appl. Phys. Lett.* **79** 3467
- [6] Ogale S B, Choudhary R J, Buban J P, Lofland S E, Shinde S R, Kale S N, Kulkarni V N, Higgins J, Lanci C, Simpson J R, Browning N D, Das Sarma S, Drew H D, Greene R L and Venkatesan T 2003 *Phys. Rev. Lett.* **91** 077205
- [7] Coey J M D, Douvalis A P, Fitzgerald C B and Venkatesan M 2004 *Appl. Phys. Lett.* **84** 1332
- [8] Hong N H and Sakai J 2005 *Physica B* **358** 265
- [9] Hong N H, Sakai J and Hassini A 2004 *Appl. Phys. Lett.* **84** 2602
- [10] Venkatesan M, Fitzgerald C B, Lunney J G and Coey J M D 2004 *Phys. Rev. Lett.* **93** 177206
- [11] Kaspar T C, Heald S M, Wang C M, Bryan J D, Droubay T, Shutthanandan V, Thevuthasan S, McCready D E, Kellock A J, Gamelin D R and Chambers S A 2005 *Phys. Rev. Lett.* **95** 217203
- [12] Dominguez J E, Pan X Q, Fu L, Van Rompay P A, Zhang Z, Nees J A and Pronko P P 2002 *J. Appl. Phys.* **91** 1060
- [13] Bryan J D, Heald S M, Chambers S A and Gamelin D R 2004 *J. Am. Chem. Soc.* **126** 11640
- [14] Radovanovic P V and Gamelin D R 2003 *Phys. Rev. Lett.* **91** 157202
- [15] Skomski R and Coey J M D 1999 *Permanent Magnetism* (Bristol: Institute of Physics Publishing)
- [16] Zaránd G and Jankó B 2002 *Phys. Rev. Lett.* **89** 047201
- [17] Pearton S J, Heo W H, Ivill M, Norton D P and Steiner T 2004 *Semicond. Sci. Technol.* **19** R59